Published in Phys. Lett. **346***(1995), pp 217-222.*

Target mass dependence of ${}^{4}_{\Lambda}$H formation mechanism from K^- absorption at rest

Y.Nara*, A.Ohnishi
Department of Physics, Faculty of Science, Hokkaido University, Sapporo 060, Japan
T.Harada
Department of Social Information, Sapporo Gakuin University, Ebetsu 069, Japan

Abstract

Formation probabilities of ${}^{4}_{\Lambda}$H from K^- absorption at rest on light nuclear targets are investigated employing antisymmetrized molecular dynamics combined with multi-step binary statistical decay. Calculated results show that as the target mass number decreases from ^{16}O, ^{12}C to ^{9}Be, the main formation mechanism varies from statistical decay, followed by dynamical fragmentation, to direct formation in nuclear environment.

key words
hyperfragment, ${}^{4}_{\Lambda}$H formation, K^- absorption at rest, microscopic transport model, Antisymmetrized Molecular Dynamics, multi-step binary statistical decay, hyperon compound nucleus

*E-mail: ynara@nucl.phys.hokudai.ac.jp , Fax: +81-11-746-5444

It has been known that various Λ hypernuclei are produced as hyperfragments from K^- absorption at rest from emulsion experiments [1]. Recently, Tamura et al. have carried out K^- absorption experiments at rest on some light nuclear targets, and they have obtained the formation probabilities of ${}^{4}_{\Lambda}$H per stopped K^- for each target from π^- spectrum of the mesonic weak decay [2]. They have also discussed the possible mechanisms of ${}^{4}_{\Lambda}$H formation with the idea of the hyperon compound nucleus [2, 3]. The calculated results show reasonable agreement with the data for ^{12}C and ^{16}O targets. However, they did not give fully satisfactory description of ${}^{4}_{\Lambda}$H formation mechanisms, by assuming the existence of equilibrated hyperon compound nuclei, which are produced in one- or two- step processes from K^- absorption prior to the fragmentation process. Therefore the dynamical properties of the primary stage of the reaction were neglected.

The aim of this study is to shed light on the fragmentation mechanism of hyperfragments from K^- absorption at rest by using a microscopic transport theory. For this purpose, we need models with which we can describe the production of hyperons and their dynamical evolution in the nucleus. One way is to apply microscopic transport models such as Boltzmann-Uehling-Uhlenbeck (BUU) model [4], Quantum Molecular Dynamics (QMD) [5, 6] and Antisymmetrized Molecular Dynamics (AMD) [7, 8], which have been standard tools for the study of heavy-ion collision problems, and which were also successfully applied to pion induced reactions [9] and $\bar{p}$ annihilation at rest [10]. These models incorporate phase space dynamics, stochastic two-body collisions, particle productions and their decays with Pauli-blocking. Among these models, AMD looks like the most appropriate one, since we can well describe in AMD the cluster structure of light nuclei, the fragmentation process and nuclear shell effects, all of which are important for the study of light hypernuclei [11]. Fragments produced in these microscopic models are, in general, in their excited states, since simulation calculations are usually truncated at some finite time. Therefore, it is necessary to take into account decays of these fragments in order to get the formation probabilities in their ground states. Combining microscopic transport models and multi-step binary statistical decay, the Kyoto group has succeeded in reproducing the production cross section of various fragments in heavy-ion reactions [6, 7]. Thus, this approach is expected to be reliable also in the hyperfragment formation reactions.

In this letter, we show the calculated results for the formation probabilities of ${}^{4}_{\Lambda}$H from K^- absorption at rest on light nuclear targets, such as ^{16}O,^{12}C,^{9}Be and ^{7}Li, and we discuss the formation mechanisms and their target dependence.

The microscopic simulation framework of AMD, which is described in detail in Ref. [7], includes two processes; classical trajectory determined by the equation of motion and the stochastic binary collision process due to the residual interaction, with Pauli-blocking. Here we briefly summarize the formulation of AMD: The wave function of the total system is given by the Slater-determinant of single-particle Gaussian wave

packets as follows;

$$\Phi = \frac{1}{\sqrt{A!}}\det[\phi_i(\xi_j)] \ , \tag{1}$$

$$\phi_i(\xi) = \left(\frac{2\nu_i}{\pi}\right)^{3/2} \exp\left[-\nu_i(\boldsymbol{r} - \boldsymbol{z}_i/\sqrt{\nu_i}) + \frac{1}{2}\boldsymbol{z}_i^2\right]\chi_i \ , \tag{2}$$

where χ_i stands for the spin-isospin wave function which is fixed in time, and the parameter ν_i represents the width of the Gaussian wave packet. For nucleon, $\nu_N = 0.16$ (fm^{-2}) is adopted, and for other baryons such as Λ and Σ, we adopt the value of $\nu_B = (m_B/m_N)\nu_N$, where m_B and m_N are masses of the baryon and nucleon, respectively. This prescription is necessary in order to remove spurious zero-point kinetic energy effects. The real and imaginary parts of the parameter $\boldsymbol{z}_i$,

$$\boldsymbol{z}_i = \sqrt{\nu_i}\boldsymbol{d}_i + \frac{i}{2\hbar\sqrt{\nu_i}}\boldsymbol{k}_i \ , \tag{3}$$

represent the mean position $\boldsymbol{d}_i$ and the mean momentum $\boldsymbol{k}_i$ of the wave packet, respectively. The equations of motion are then obtained by applying the time-dependent variational principle (TDVP):

$$i\hbar\sum_j C_{ij}\dot{\boldsymbol{z}}_j = \frac{\partial\mathcal{H}}{\partial\bar{\boldsymbol{z}}_i} \ . \tag{4}$$

We note that there appears a matrix $\boldsymbol{C}$ which modifies the equations of motion to non-canonical form. This matrix comes from the anti-symmetrization of the wave function.

We use the following effective interactions in this work. For N-N, the effective interaction Volkov No.1 [12] with Majorana parameter $m = 0.65$ is used. In order to fit the binding energies of normal nuclei up to ^{16}O and to remove spurious zero-point kinetic energy of fragments, the zero-point kinetic energy correction term is added to the Hamiltonian in the same way as Ref. [8]. For N-Λ interaction, we choose the one range Gaussian potential,

$$v_{N\Lambda} = v_0(w + mP_r)\exp(-r^2/\lambda^2), \tag{5}$$

$$v_0 = -43.622\text{MeV}, \quad m = 0.9, \quad w = 1 - m, \quad \lambda = 1.034\text{fm}, \tag{6}$$

where the strength of this potential and Majorana parameter are considered as free parameters to fit the experimentally known binding energies of various light Λ hypernuclei, and the range is the same as that of two pion exchange [11]. For N-Σ effective interaction, we use Harada one range Gaussian (H1G) potential, which is newly developed here,

$$v_{N\Sigma} = [v_0 + v_\sigma(\boldsymbol{\sigma}_N\cdot\boldsymbol{\sigma}_\Sigma) + v_\tau(\boldsymbol{\tau}_N\cdot\boldsymbol{T}_\Sigma) + v_{\sigma\tau}(\boldsymbol{\sigma}_N\cdot\boldsymbol{\sigma}_\Sigma)(\boldsymbol{\tau}_N\cdot\boldsymbol{T}_\Sigma)]\exp(-r^2/\mu^2) \ , \tag{7}$$

where $\mu = 1.0\text{fm}, v_0 = -7.7075\text{MeV}, v_\sigma = 9.1275\text{MeV}$, and $v_\tau = v_{\sigma\tau} = 18.255\text{MeV}$. This potential is obtained so as to reproduce the characteristic features of $A = 4$ Σ hypernuclei [13].

Table 1:
Branching ratio for K^- absorption at rest obtained from K-matrix formalism [14]. Fermi average and binding effect are considered. We have used 20 MeV for ^{7}Li and ^{9}Be, 12.5 MeV for ^{12}C and 8 MeV for ^{16}O.

B_N	20 MeV	12.5 MeV	8 MeV
$K^-p \to \Lambda\pi^0$	0.029	0.050	0.070
$K^-n \to \Lambda\pi^-$	0.058	0.100	0.140
$K^-p \to \Sigma^-\pi^+$	0.318	0.334	0.313
$K^-p \to \Sigma^0\pi^0$	0.256	0.204	0.156
$K^-p \to \Sigma^+\pi^-$	0.243	0.154	0.106
$K^-n \to \Sigma^-\pi^0$	0.048	0.079	0.108
$K^-n \to \Sigma^0\pi^-$	0.048	0.079	0.108

The initial condition is given as follows; first, for nucleon momentum, after transforming to physical variables [7], momentum fluctuation of the Gaussian wave packet, $(\Delta p_N)^2 = \hbar^2\nu_N$, is generated randomly. Recoil effects are taken into account in order to conserve the total momentum. Then in the same way as the ordinary two-body collision term of AMD, momenta of π meson and $Y(=\Lambda$ or $\Sigma)$, are determined in the reaction of $K^- + N \to \pi + Y$, where the branching ratios are determined from the K-matrix formalism [14], including a Fermi average with binding effects. Parameters and the calculated branching ratios are shown in Table I.

Branching ratio of two body absorption processes $K^-NN \to YN$ for ^{12}C target has been known experimentally to be about 19% [15], however, it is difficult for the produced hyperons to stop in target nuclei because of their large momentum($\sim$ 600 MeV/c). Therefore we ignore these two nucleon absorption processes, while the modification of normalization is taken into account by reducing ${}^{4}_{\Lambda}$H formation probability by 20% (see fig. 4).

One needs also elementary cross sections of baryon-baryon collisions. The following elementary collisions are put into our calculations: (1) $N+N \to N+N$, (2) $N+\Lambda \to N+\Lambda$, (3) $N+\Sigma \to N+\Sigma$, (4) $N+\Sigma \leftrightarrow N+\Lambda$, where $N = n, p$ and $\Sigma = \Sigma^-, \Sigma^0, \Sigma^+$. The parametrizations of experimental cross section (2)$\sim$ (4) are taken from Ref. [16]. The different isospin channels are taken into account using the respective Clebsh-Gordan coefficients.

We have made AMD simulation calculation of K^- absorption at rest on ^{16}O, ^{12}C, ^{9}Be and ^{7}Li targets. Calculated number of events is 2000 for each reaction, and the time-evolution until t = 200 fm/c from K^- absorption is calculated. The time-step for the equation of motion is chosen to be 1.0 fm/c. For the accuracy in the time-development, we have used the Heun method, which is a kind of second order Runge-Kutta method.

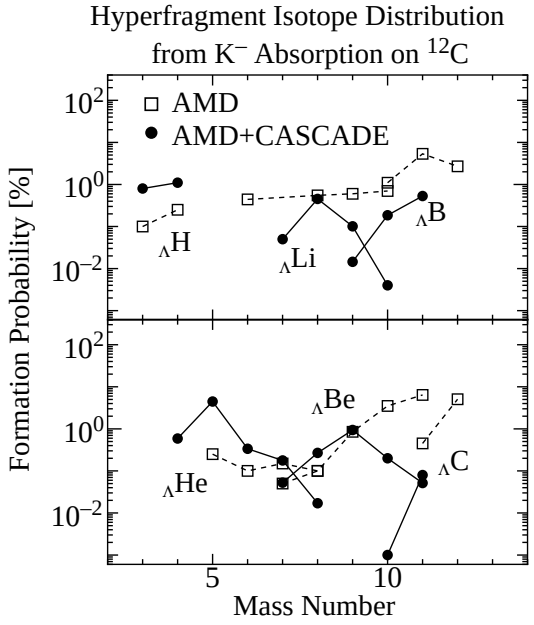

Figure 1:
Hyperfragment isotope distribution from K^- absorption at rest on ^{12}C. Boxes are the results of AMD calculation and black circles are the results after the multi-step statistical decay calculation.

Hereafter, we discuss the results of ^{12}C target case in detail. The calculated hyperfragment isotope distribution of this reaction is shown in fig. 1 (dashed lines). The total probability of *excited* hyperfragment formation amounts to about 29 %. Mass distribution of $A \leq 10$ hyperfragments produced in AMD is about one-third of the total yield of the hyperfragments and the rest is the contribution of hyperon compound nuclei with mass number $A = 11$ and 12.

The excitation energies of these hyperfragments are around $30 \sim 40$ MeV, and these fragments decay statistically. Therefore, we input the excitation energies and angular momenta of the produced fragments in the CASCADE code which is essentially the same version used in Ref. [6] with some modification in order to treat hyperfragments. Modifications from that of Ref. [6] are as follows. (1) Binding energies of hypernuclei are taken from experimental data if possible, and if it is not possible, we add the calculated separation energy of Λ in AMD to the binding energy of normal nuclei. (2) Excitation levels of ${}^{4}_{\Lambda}$He and ${}^{4}_{\Lambda}$H are included.

After carrying out multi-step binary statistical decay calculation for these excited hyperfragments, we have got the hyperfragment formation probabilities in their *ground states*, which will be detected in the experimental measurement. In fig. 1, we also show the results of hyperfragment distribution in the framework of AMD+CASCADE (solid lines). Calculated result shows good agreement with the data of ${}^{4}_{\Lambda}$H formation ($\sim 1\%$).

To clarify the formation mechanism of ${}^{4}_{\Lambda}$H, it is worthwhile to examine the parent hyperfragment distribution of ${}^{4}_{\Lambda}$H in the statistical decay. In fig. 2, we show the parent hyperfragment distribution of ${}^{4}_{\Lambda}$H. We note from fig. 2 that the sources of ${}^{4}_{\Lambda}$H are dynamically produced neutron rich hyperfragments, and their mass numbers widely

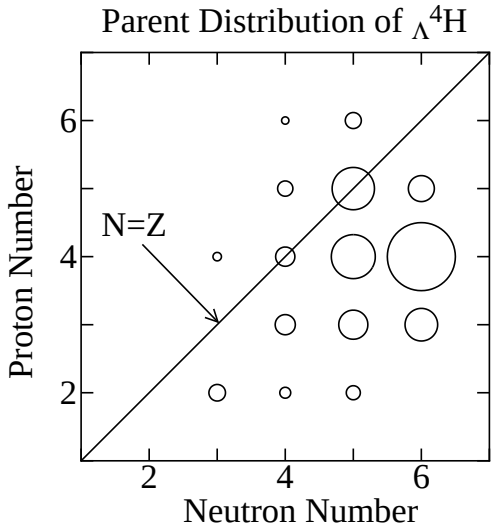

Figure 2:
Parent hyperfragment distribution of ${}^{4}_{\Lambda}$H from K^- absorption at rest on ^{12}C. The area of the circle is proportional to the probability from that hyperfragment.

range from 6 to 12. This result gives a slightly different picture from *hyperon compound nucleus* proposed in Ref. [2]. In Tamura's work, the sources of ${}^{4}_{\Lambda}$H are limited to hyperon compound nuclei with mass number 11 and 12, and they have estimated the formation probability of ${}^{4}_{\Lambda}$H to be about $0.24 \sim 0.67$ %. In this work, although the contribution from these hyperon compound nuclei amounts to about 0.6%, it is found that hyperfragments with $A \leq 10$ make non negligible contributions to the formation rates of ${}^{4}_{\Lambda}$H (~ 0.5 %), and their sum becomes the total yield (~ 1 %). Thus the dynamical fragmentation or nucleon emission in the primary stage due to multi-step processes is indispensable for quantitative arguments.

We show in fig. 3 the results of hyperfragment mass distribution in the case of ^{16}O target, together with ^{12}C target. The calculated formation probability of ${}^{4}_{\Lambda}$H is about 0.37 %, and well coincides with the experimental data (~ 0.47 %). However, the formation mechanism is somewhat different from that in the case of ^{12}C target, since there appear no small hyperfragments in the dynamical stage. Therefore, the sources of ${}^{4}_{\Lambda}$H are *heavy* hyperon compound nuclei, and this indicates almost the same picture as that of *hyperon compound nucleus*.

The target dependence of ${}^{4}_{\Lambda}$H formation are summarized in fig. 4. As is already discussed above, AMD+CASCADE results well reproduce the experimental data for ^{16}O and ^{12}C. However, in the lighter target cases such as ^{9}Be and ^{7}Li, AMD+CASCADE approach underestimates ${}^{4}_{\Lambda}$H formation probabilities. Since these lighter targets have the cluster structure in their ground states (^{9}Be has the α+α+n structure and ^{7}Li has the α-t structure). and are easy to break up to α particle or some other s-shell nuclei, it is quite difficult to produce hyperon compound nuclei.

Alpha clustering in the ground states of light targets suggest the importance of *direct* production of ${}^{4}_{\Lambda}$H from K^- absorption by the α particle in the target. The direct formation probability of $K^- + \alpha \rightarrow \pi^0 + {}^{4}_{\Lambda}$H amounts to about 1 %, and it is expected

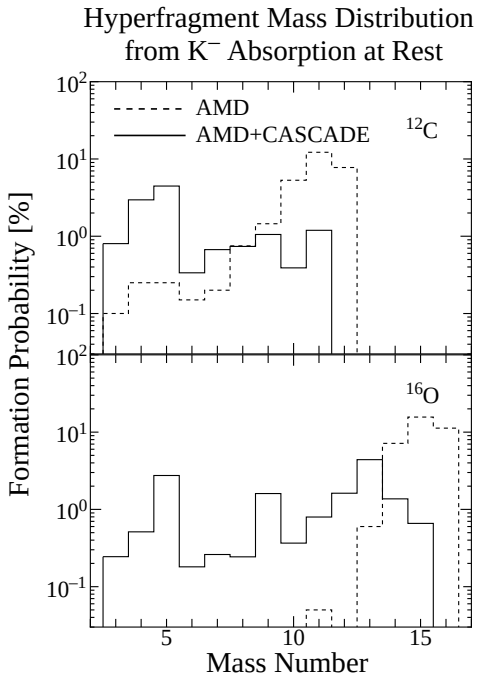

Figure 3:
Hyperfragment mass distributions from K^- absorption at rest on ^{12}C and ^{16}O. Dashed and solid histograms represent results of AMD calculation and after the multi-step statistical decay calculation, respectively.

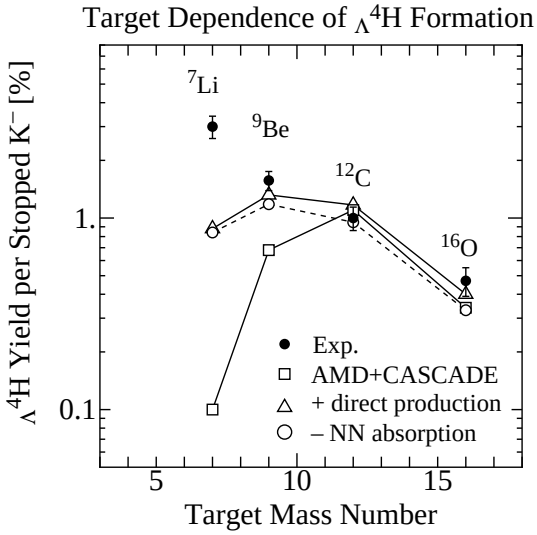

Figure 4:
Target mass dependence of $^4_\Lambda$H formation probabilities. Boxes and triangles with solid lines represent AMD+CASCADE results without and with direct $^4_\Lambda$H production. White circles with dotted line show the results with direct production while AMD+CASCADE results are reduced by 20 % (see text). We also show the experimental data (black circles with error bars) taken from Ref. [2].

that a large part of these directly produced ${}^{4}_{\Lambda}$H nuclei in the target escape from the reaction region because of the cluster structure. Usually, this type of direct production process is not included in microscopic transport models, since coherent effects such as many-body correlations and recoil cannot be treated in the framework of two-body collision process.

From this point of view, we have simply estimated the survival probability of directly produced ${}^{4}_{\Lambda}$H nuclei in the target by the use of the Glauber model. It is assumed that the target nuclei have cluster structure of α-t and α-α-n for ^{7}Li and ^{9}Be, respectively. Distances between these clusters are determined to fit the r.m.s. radii, and anti-symmetrization is ignored at this moment. After the direct production of ${}^{4}_{\Lambda}$H from one of the α particle in the target, the survival probability of this ${}^{4}_{\Lambda}$H is calculated from the integral of density overlap along the escaping path;

$$P(\text{survival}) = \int \frac{d\hat{e}}{4\pi} \exp(-\chi(\hat{e})), \tag{8}$$

$$\chi(\hat{e}) = \int_0^\infty dz \int d\boldsymbol{r}\ \sigma\ \rho_1\ (\boldsymbol{r} - \boldsymbol{r}_1 - z\hat{e})\ \sum_{i\neq 1} \rho_i(\boldsymbol{r})\ , \tag{9}$$

where $\rho_i(\boldsymbol{r})$ represents the baryon density in the i-th cluster, and $\boldsymbol{r_1}$ is the formation point of ${}^{4}_{\Lambda}$H (first cluster). The cross section is chosen to be 40 mb.

Calculated direct production and survival probabilities added to the AMD + CASCADE results are shown in fig. 4. Both in the case of ^{9}Be and ^{7}Li targets, we have found that direct contribution cannot be ignored, i.e., comparable or larger to the AMD+CASCADE results. For ^{9}Be target, the sum of these two contribution well coincides with the experimental data. For ^{7}Li target, although the absolute value of the probability is still smaller than the experimental data, the addition of direct contribution largely remedies the problem.

We have also applied the above simple estimation to the ^{12}C and ^{16}O target reactions, assuming that they have 3-α and 4-α structures. This simple estimation is expected to overestimate the probability since these nuclei have the shell model structure rather than α-clustering structure. However, the contribution of direct process is calculated to be much smaller than that of AMD+CASCADE results.

As already mentioned, we ignore two nucleon absorption branches, then we need to reduce AMD+CASCADE results by about 20 % to take account of the modification of normalization. These results with direct contributions are shown in fig. 4 (white circles), however, we can not see any significant effects under our assumption.

In summary, the formation probabilities of hyperfragments have been investigated with the AMD simulation and CASCADE statistical decay approach. Calculated results show that the formation probabilities of ${}^{4}_{\Lambda}$H on the targets of ^{16}O, ^{12}C and ^{9}Be are well explained if we take the *direct* production process into account. However, the experimental large formation probability of ${}^{4}_{\Lambda}$H on ^{7}Li target (3 %) remains a mystery. One of the reasons might be that the AMD wave function used here does not show the proper clustering structure of α-t, since the parity projection of the target nucleus is

ignored.

The formation mechanism of ${}^{4}_{\Lambda}$H depends strongly on the target nuclei and it contains various and rich processes, from direct production in nuclear environment, followed by dynamical fragmentation, to statistical decay of highly excited hyperon compound nuclei. We have found that this dependence comes from the structure of target nuclei, namely, the formation mechanism largely depends on whether the target nucleus has α-clustering structure or not. From these analyses, we find that the dynamical model approach of AMD+CASCADE, which has succeeded in heavy-ion reactions, is also powerful for the kaon induced reaction and the formation mechanisms of hyperfragments.

In this work, we have not calculated the explicit propagation of mesons. It is interesting to investigate the effect of pion rescattering or absorption. The main effect is probably to provide more energy to the various fragments which come out of the compound nucleus, thereby, changing the dynamical fragmentation pattern. We are now studying these effects, by including pion-nucleon interaction and delta propagation in the same way as in Ref. [9]. Preliminary results [17] with π-N intereaction suggest the formation mechanism of ${}^{4}_{\Lambda}$H is similar to that proposed in this letter.

The authors thank Prof. M. Sano, Dr. H. Tamura and Prof. K. Katō for valuable comments and discussions. The calculations in this work were financially supported in part by Research Center for Nuclear Physics (RCNP), Osaka University, as RCNP Computational Nuclear Physics Project No. 93-B-03.

References

[1] D. H. Davis and J. Sacton, *High Energy Physics*, edited by E. H. S. Burhop (Academic, New York,1967), Vol.II, p.365.

[2] H. Tamura *et al.*, Phys. Rev. **C40** (1989) R479, R483.

[3] T. Yamazaki, Nuovo Cimento **103A** (1989) 78.

[4] G. F. Bertsch and S. Das Gupta, Phys. Rep. **160** (1988) 189;
W. Cassing, V. Metag, U. Mosel and K. Niita, Phys. Rep. **188** (1990) 363.

[5] J. Aichelin, Phys. Rep. **202** (1991) 233.

[6] T. Maruyama, A. Ono, A. Ohnishi and H. Horiuchi, Prog. Theor. Phys. **87** (1992) 1367.

[7] A. Ono, H. Horiuchi, T. Maruyama, and A. Ohnishi, Prog. Theor. Phys. **87** (1992) 1185; Phys. Rev. Lett. **68** (1992) 2898; Phys. Rev. **C47** (1993) 2652.

[8] A. Ono, H. Horiuchi and T. Maruyama, Phys. Rev. **C48** (1993) 2946.

[9] A. Engel, W. Cassing, U. Mosel, M. Schäfer and Gy. Wolf, Nucl. Phys. **A572** (1994) 657.

[10] J. Cugnon, P. Jasselette and J. Vandermeulen, Nucl. Phys. **A470** (1987) 558.

[11] T. Motoba, H. Bandō, K. Ikeda and T. Yamada, Prog. Theor. Phys. Suppl. No.**81** (1985), Chap. III.

[12] A. Volkov, Nucl. Phys. **75** (1965) 33.

[13] T. Harada, Nucl. Phys. **A547** (1992) 165c.

[14] A. D. Martin, Nucl. Phys. **B179** (1981) 33.

[15] C. D. Vander *et al.*, Nuovo Cimento **39A** (1977) 538.

[16] J. Cugnon, P. Deneye and J. Vandermeulen, Phys. Rev. **C41** (1990) 1701.

[17] Y. Nara, A. Ohnishi and T. Harada, in preparation.